The International Journal of Advanced Manufacturing Technology (2023) 124:1065–1076
https://doi.org/10.1007/s00170-022-10214-2

ORIGINAL ARTICLE

Influence of oxygen content in the shielding gas chamber on mechanical properties and macroscopic structure of Ti-6Al-4V during wire arc additive manufacturing

Christoph Halisch[1] · Björn Milcke[2] · Tim Radel[1] · Rüdiger Rentsch[3] · Thomas Seefeld[1]

Received: 15 June 2022 / Accepted: 27 September 2022 / Published online: 28 November 2022

Abstract
Wire arc additive manufacturing (WAAM) of titanium parts shows promising potential for aerospace application due to its high deposition rates allowing a fast and economical production of large components. The cost savings are high, especially for expensive alloys like Ti-6Al-4V. However, due to high oxygen affinity of Ti-6Al-4V at elevated temperatures an excellent shielding gas coverage seems necessary to prevent embrittlement of the material during the welding process. Regarding the future development of local shielding gas coverage set-ups for gas metal arc welding (GMAW) based WAAM, this study investigates the influence of the oxygen content in the shielding gas chamber on mechanical properties of Ti-6Al-4V during the welding process. Samples are welded at different oxygen contents in the shielding gas chamber and stress-relief heat treated afterwards. Inert gas milling and hot gas extraction are used to determine the material oxygen content at different deposition heights. Metallographic methods are used to show macroscopic grain structure, evaluate possible α-case thickness and its dissolution by the subsequent layer. Hardness testing is used to investigate possible material inhomogeneities in the deposit and tensile properties of the material welded at different chamber oxygen contents are displayed. It is concluded, that even at high chamber oxygen levels of 6000 ppm the welding process is stable, the forming α-case at top of the layer dissolves in the melt pool of the subsequent layer and that the aerospace requirements on tensile properties can be reached.

Keywords Additive manufacturing · DED · GMAW · Mechanical properties · Microstructure · Oxygen · Ti-6Al-4V · WAAM

1 Introduction

Wire arc additive manufacturing (WAAM) offers a multitude of potentials not solely towards key engineering materials like nickel alloys [1], steels [2], and others, but to new materials like shape alloys [3] or graded materials [4] as well. One of the advantages of additive manufacturing processes is the possibility to produce near net-shape parts with a high material usage efficiency. For large-scale titanium parts, WAAM shows promising potential due to its high deposition rates. Especially for expensive alloys like Ti-6Al-4V, the cost savings are high. The requirement for a widespread industrial application is a robust deposition process ensuring reproducible mechanical material properties. One influence factor on the material properties of titanium alloys like Ti-6Al-4V is the amount of oxygen pick-up during welding and dissolving into the material, which can lead to an embrittlement of titanium alloys [5]. ASTM Grade 5 Titanium (Ti-6Al-4V) has a maximum allowable oxygen content of 2000 ppm. At elevated temperatures, titanium alloys have a high affinity to picking up oxygen from the surrounding atmosphere. Therefore, Ti-6Al-4V parts manufactured by WAAM are often produced within highly covered shielded gas atmospheres to prevent material embrittlement [6]. While other publications [7–10] usually cover the influence of ambient air, which in addition to oxygen contains nitrogen and hydrogen that cause embrittlement as well, this work covers the separated influence of oxygen alone on

✉ Christoph Halisch
halisch@bias.de

[1] BIAS - Bremer Institut Für Angewandte Strahltechnik GmbH, Klagenfurter Str. 5, 28359 Bremen, Germany

[2] Airbus Operations GmbH, Airbus-Allee 1, 28199 Bremen, Germany

[3] IWT - Leibniz-Institut Für Werkstofforientierte Technologien, Badgasteiner Str. 3, 28359 Bremen, Germany

Table 1 Chemical analysis of the Ti-6Al-4V wire (source: Perryman data sheet)

Element	Ti	Al	V	Fe	O	Si	N	H
Content (wt-%)	Balance	6.39	3.96	0.18	0.16	0.011	0.007	0.003

the mechanical properties of Ti-6Al-4V during the WAAM process.

The reactivity of Ti-6Al-4V with oxygen increases with rising temperatures exceeding 550 °C as does the speed of the oxidation process [11]. Unlike pure titanium, Ti-6Al-4V forms both Al_2O_3 and TiO_2 under oxygen atmosphere and the oxidation kinetics obeys the parabolic law. The TiO_2 layer grows fast and has a strong disordered lattice structure which is not very protective against further oxidation, while Al_2O_3 layers are more protective [12]. This means the oxidation rate decreases over time due to the slower diffusion through the growing oxide layer [13]. The oxidation rate is dependent on the temperature, time, microstructure, and atmospheric pressure.

During welding, oxygen can find its way into the material through the weld pool or hot areas in the weld trail, where the diffusion capability is high [7]. However, the potential to pick up significant amounts of oxygen is higher through the melt pool due to the higher temperature, the higher diffusion coefficient in the liquid state as well as constant material transport away from the surface due to melt pool convection [14]. Due to layer-based material deposition during WAAM, the deposit undergoes repeated reheating [6, 15] by the subsequent layer that enables continued oxidation.

Strategies for local protection include multiple gas nozzles and sometimes barriers attached to the welding torch, creating an inert gas stream that protects critical areas. Ding et al. developed a local shielding, approaching a non-turbulent gas flow [9]. However, in local shielding during WAAM, the atmosphere still contains oxygen [7, 9].

In chamber shielding, an appropriate oxygen content in the process environment may require a long purging time with inert gas, depending on the gas injection strategy [9]. In a study conducted by Elmer et al. it is reported, that WAAM deposits processed under air atmosphere show oxygen contents which are above specification levels [8]. However, when they mixed an argon atmosphere with air and the oxygen content in the chamber reached around 850 ppm, they reported an average oxygen content in the deposit that was approximately 100 ppm over the welding wire's oxygen content. According to the research of Ding et al. no significant changes in the hardness occur where the oxygen content is less than 4000 ppm or conservatively 2000 ppm [9], which was not to be expected following the state of the art at that time. Caballero et al. [10] confirmed, those tensile properties are not compromised by an increase of oxygen in the shielding environment up to 4000 ppm and additionally found, that high temperatures and exposure times seem to have a greater effect on oxidation than oxygen content in the shielding environment.

If the level of oxygen can be modeled precisely, it can be used as a strengthening mechanism to increase the load-bearing capacity of the material [14]. As of today, the influence of oxygen and nitrogen on the mechanical material properties of in WAAM has been examined using ambient air and therefore, a distinction between the effects of oxygen and nitrogen onto the material properties is not possible. The novelty this paper presents is the investigation of the separated influence of pure oxygen content rather than ambient air in the shield gas chamber on mechanical properties of Ti-6Al-4V during the WAAM process.

2 Materials and set-up

2.1 Materials

A Ti-6Al-4V wire with a diameter of 1.2 mm was used. The chemical analysis according to the supplier is shown in Table 1.

Pickled Ti-6Al-4V plates with a size of 200 mm × 80 mm × 10 mm were used as substrate material. The chemical analysis of the substrate material is shown in Table 2.

2.2 Oxidation of the substrate surface

While most specimen were welded on pickled Ti-6Al-4V plates, the surface of a few substrate plates was purposefully oxidized using a 1080 nm JK400FL single-mode Ytterbium fiber laser. A beam attenuator was used leading to a laser power of 41 W. A telocentric f-theta optic was used for focusing and a scanning system (Raylase Superscan III-15) was used for guiding. The focal diameter was 110 µm. The substrate material is moved using a two-axis positioning table while the laser remains in a fixed position. A first

Table 2 Chemical analysis of the Ti-6Al-4V base material (source: GAB titan data sheet)

Element	Ti	Al	V	Fe	O	Si	N	H
Content (wt-%)	Balance	6.20	4.08	0.17	0.15	-	0.01	0.002

hatch pattern with hatch distance of 35 µm was placed onto the substrate material. A second hatch pattern was placed orthogonally onto the first hatch pattern to ensure homogenous oxidation. The specimen was irradiated in a field of 20 mm × 30 mm. The scanning velocity was set from 1100 to 50 mm/s resulting in increasing surface temperatures and increasing in oxide layers thickness in the air atmosphere. Judging by the visual discoloration on the titanium substrate surface, the oxide layer thickness is uniform along the irradiated area and its thickness can be easily be controlled by the method.

2.3 Welding process

The welding experiments were performed with a Gefertec Arc403 3D metal printing machine. This machine contains a Fronius TransPuls Synergic 4000 CMT R power source which is mounted on a three-axis gantry system. The arc mode was CMT at a wire feed rate of 9.8 m/min, a nominal current of 179 A, a nominal voltage of 16.6 V, and a travel speed of 1.8 m/min. A mixture of 70% Helium and 30% Argon (ArHe 30/70) was used as process gas with a flow rate of 16 l/min. The distance between workpiece and contact tip was set to 15 mm. As shown in Fig. 1, a shielding gas chamber was used to control the oxygen content in the atmosphere during processing. This chamber was filled with Argon 4.8 (purity 99,998%) and varying amount of ArO 98/2 mixture. While increasing the amount of ArO 98/2, the amount of pure Argon was reduced, resulting in a constant total flow rate of 30 l/min. The oxygen content in the shielding gas chamber was monitored before and during welding using amperometric oxygen sensors with 100–10000 ppm and 1000–250000 ppm range. The welding process was started after a purge time of 15 min. Samples with a width of 22 mm, a length of 198 mm, and a height of 120 mm were deposited. In every second layer, the starting and end point were switched. Between each layer, a dwell time of 120 s was maintained. The welding head was oscillated with a meander motion. Samples with the mentioned welding parameters were welded with varying ArO_2 98/2 flow rates resulting in different oxygen contents in the shielding gas atmosphere. When welding on preoxidized substrate material, single walls without meander torch movement were deposited.

2.4 Heat treatment

The samples were cut into two sections and one section of each sample was heat treated for 2.5 h at 650 °C in an oven constantly purged with 10 l/min of Argon 4.8 gas. This temperature regime is commonly chosen within aerospace industry to relieve the thermal stress of Ti-6Al-4V and its influence on the tensile properties has been previously investigated [16]. The heat-treated section was used for hardness and tensile testing. The as-built section was used for hot gas extraction and metallographic analysis.

2.5 Inert gas milling

Milling chips were extracted at different heights shown in Fig. 2 to analyze the oxygen content within the material. A carbide milling tool with a SiTiN coating, 3 cutting edges, and a diameter of 6 mm was used. The machining chamber was continuously purged with Argon 4.8 to suppress oxide exposure of the generated chips as much as possible at high local process temperatures. First, a material layer of about

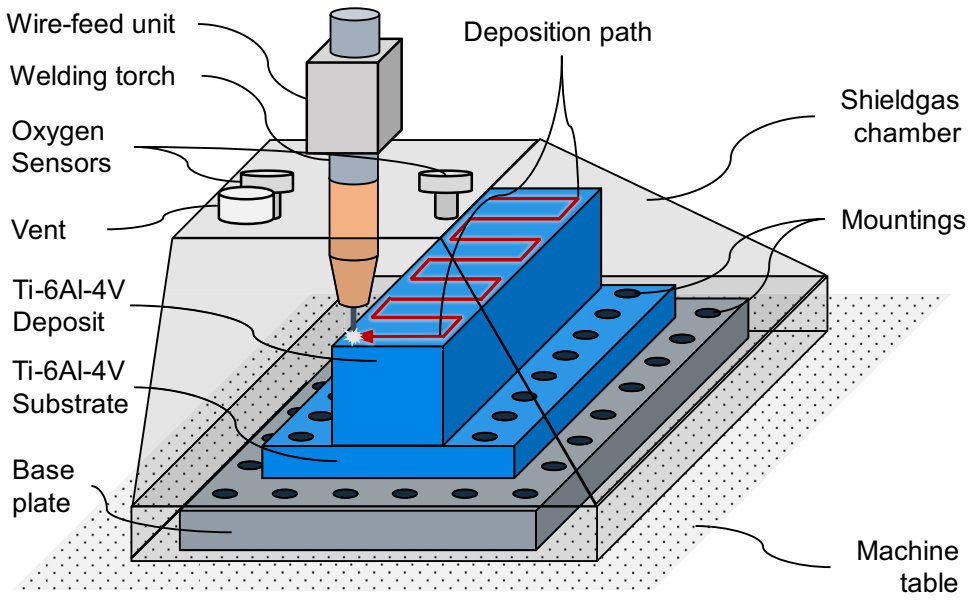

Fig. 1 Experimental set-up

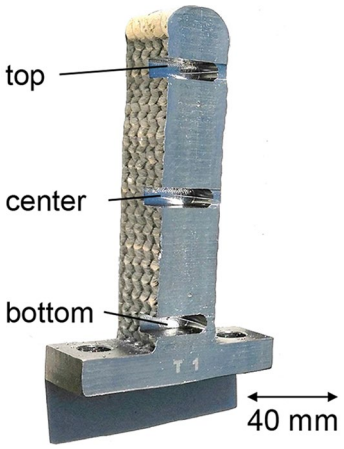

Fig. 2 Extractions of milling chips at different heights from samples welded with different oxygen content in shielding gas chamber

2 mm thickness was machined off the surfaces to eliminate surface effects. Then a series of face milling operations was conducted at 1500 rpm and axial feed of 200 mm/min with a radial displacement of 0.8 mm each. The chips were collected in small glass containers filled with Argon and transferred directly to the hot gas extraction. The milling chips were extracted at different heights: bottom (5 mm from substrate material), center (50 mm from substrate material), and top (100 mm from substrate material). Three samples welded at different chamber oxygen contents (200 ppm, 1000 ppm, 6000 ppm) were examined. To serve as a reference, the substrate material was milled using the described method and a welding wire specimen was taken directly from stock material. Before the analysis of the TiAl6V4 welding wire, the surface was cleaned by SiC abrasive paper to remove possible contaminations off the surface.

2.6 Hot gas extraction

The oxygen contents dissolved in the material were evaluated using hot gas extraction using an ELTRA ONH 2000. After cleaning the process chamber and the graphite crucible by heating with 6 kW and continuous rinsing with Helium as carrier gas, the material sample is transferred into the crucible. For better processing and to enhance outgassing, the small Ti-6Al-4V milling chips were filled in Ni capsules and molten together. The possible intake of additional oxygen by the Ni capsules was assessed and data was corrected. The sample mass was about 60 mg each and measurements were repeated 3 to 5 times.

2.7 Metallographic analysis

The cross sections were ground, polished, and etched. The etchant used was a Kroll etchant. The thickness of α-case has been measured at five different locations in the region of interest, as the maximum of these values is given as thickness of α-case.

2.8 Hardness testing

Hardness testing was conducted following the DIN EN ISO 6507–1 using a Struers DuraScan 50 G5 automated hardness testing machine. Vickers hardness HV 1 was tested with a spacing in between indentations of 250 µm or 500 µm and the results of five parallel lines were averaged.

2.9 Tensile testing

Tensile test specimens were extracted from the sample parallel to build up direction according to Fig. 3 using wire cut EDM. Their dimensions comply with the ASTM E8 flat tensile specimen type No. 2 (H = 4 mm, L = 91 mm, W = 15 mm). The tensile strength specimens were extracted in 5 mm distance to the interface of substrate material and welded material. A total of 10 tensile specimen were tested for each welded sample using an Instron 1185 SN according to EN 2002–1 test method at 23 °C/50% RH with 0.5 // 5 mm/min test speed.

3 Results

As shown in Fig. 4, the average chamber oxygen content during welding increases with higher ArO_2 98/2 gas flow. A recurring periodic change of chamber oxygen content can be observed, while the amplitude increases with higher ArO_2 98/2 gas flow. Even though periodic changes occur, the average chamber oxygen content decreases over the weld time until it reaches a constant level. For simplification, the

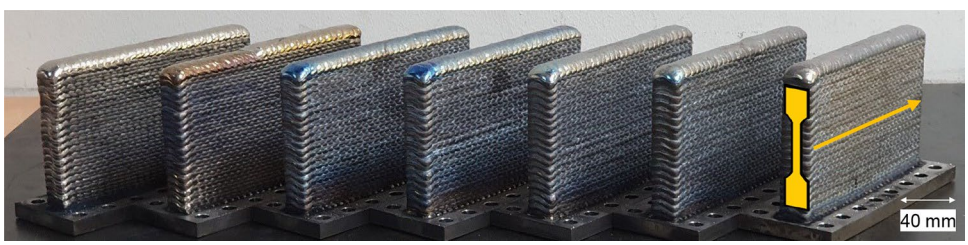

Fig. 3 Welded samples and indicated placement of tensile specimen

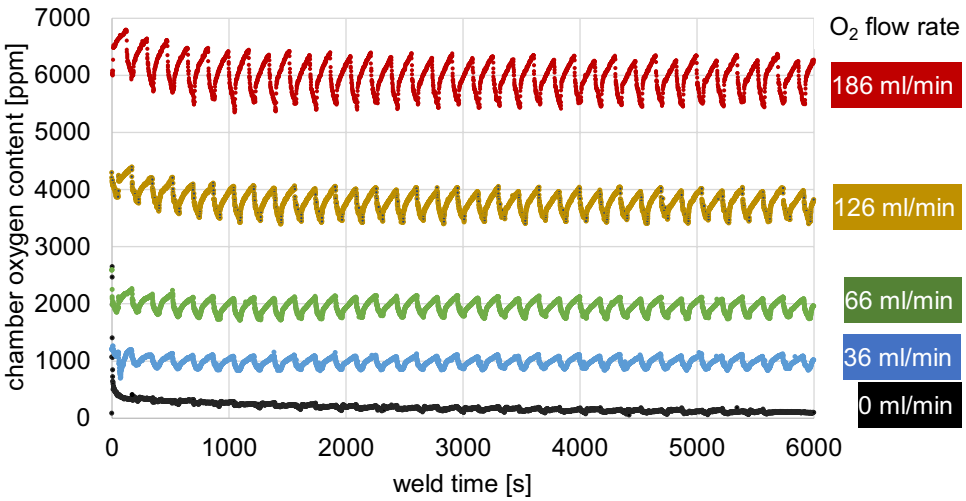

Fig. 4 Chamber oxygen content during welding depending on different oxygen flow rate

samples welded using different ArO_2 98/2 gas flow levels (0 // 1.2 // 2.2 // 4.2 // 6.2 l/min) will be referred to by the respective resulting average chamber oxygen content (200 // 1000 // 2000 // 4000 // 6000 ppm).

Upon removing the samples from the shielding gas chamber after welding, different visual discolorations depending on the chamber oxygen content can be observed as shown in Fig. 5. The visual discolorations on top of the welded samples change from metallic silver, blue-violet, light blue, and matt gray with increasing oxygen contents in the shielding gas chamber, which indicates different thicknesses of oxide layers on the welded samples. The same change in visual discolorations can be observed when changing the laser scanner velocity and the resulting different heat input during preoxidizing of a few of the substrate materials shown in Fig. 6, which were used for single wall deposition only.

The changing visual discolorations in correlation to the chamber oxygen content are shown in Fig. 5, the likewise change of the visual discolorations over the deposition height is shown in Fig. 7. The visual discolorations changes from a golden, a blue, a light blue to a matt gray color indicating an increasing oxide layer thickness over the deposition height. In comparison to the weld start and end, the change in visual discolorations indicates thicker oxide layer in the center of the sample.

The oxygen contents measured in the bulk material of the deposit, the wire, and the substrate material are shown in Fig. 8. The substrate material shows a lower oxygen content in comparison to the welding wire stock material. When comparing the material oxygen content within one welded specimen at different build-up heights, a trend can be observed. The oxygen content in the material close to the substrate material (bottom) is lower compared to the oxygen content in the material of the last layers (top) and between (center). The oxygen content in the welded material in between (center) shows the highest oxygen content. When welding at low chamber oxygen content (200 ppm), the material oxygen content close to the substrate (bottom) is lower than the material oxygen content of the wire feedstock. If the chamber oxygen content increases, the material oxygen content increases as well. However, when drastically changing the chamber oxygen contents, the change in material oxygen content in relation is lower than expected. It needs to be noted, even when welding at low chamber oxygen content, the chemical requirements of the ASTM titanium grade 5 with a maximum allowed oxygen content of 2000 ppm will be exceeded in the center of the deposit.

Unexpectedly, the hardness profiles along the width of the deposit shown in Fig. 9 do not change significantly, neither in correlation to the oxygen contents in the

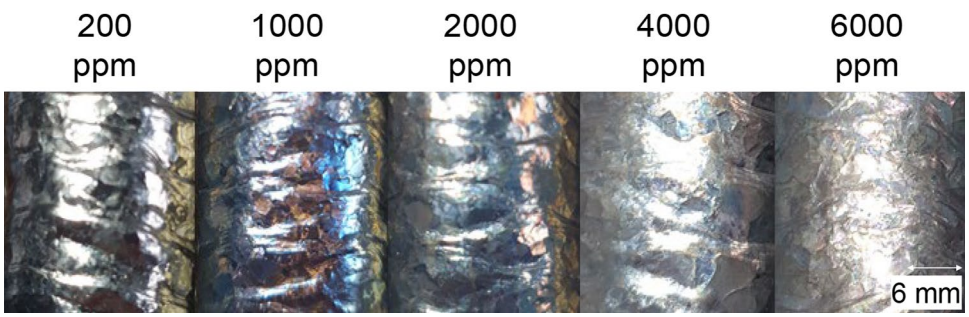

Fig. 5 Visual discolorations depending on different chamber oxygen contents

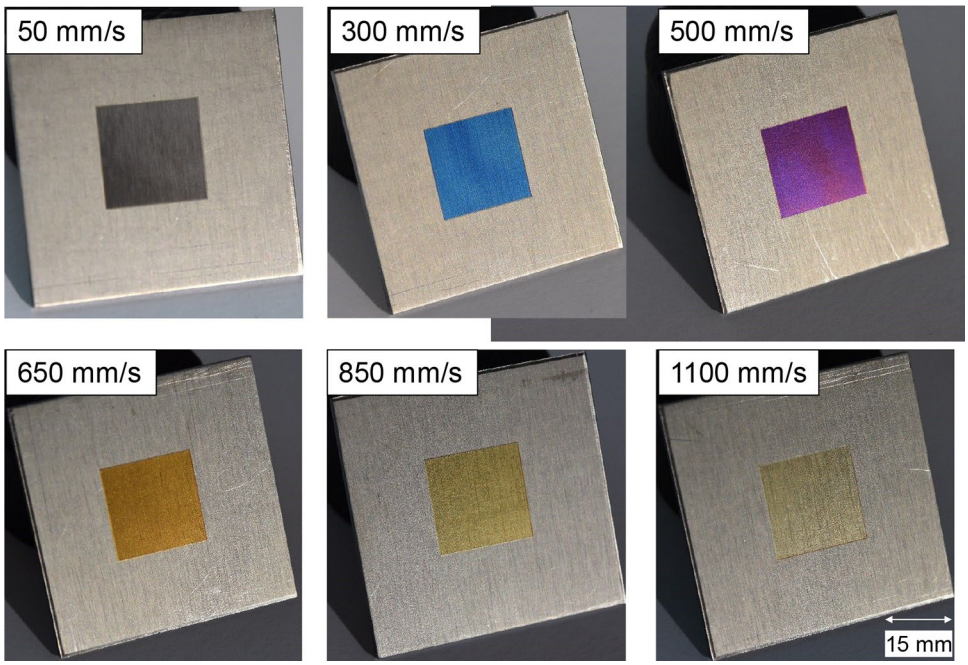

Fig. 6 Visual discolorations of Ti-6Al-4V substrate material preoxidized using laser heating at different laser scanning velocities

shielding gas chamber nor in correlation to the distance from the center of the sample. Standard deviations, which are not displayed for the purpose of clarity, as well as the measurement inaccuracy of hardness testing, predominate the observed slight differences.

Figure 10 shows the hardness profiles along the height starting from the center of the top layers surface. Unlike the hardness profile along the width of the samples shown in Fig. 9, a periodical increase of approximately 15 HV in the samples welded at high chamber oxygen levels (6000 ppm) can be observed along the height of the deposit. The periodicity correlates to the layer height of 2.5 mm.

The results of static tensile testing are shown in Fig. 11. With increasing chamber oxygen contents the yield strength and tensile strength increase, while the elongation after fracture decreases. The sample welded at 200 ppm chamber oxygen content does not follow the said trend when comparing the elongation after fracture. Even samples welded at high chamber oxygen contents of 6000 ppm will reach the tensile test requirements from the aerospace industry indicated with dashed lines in Fig. 11. However, as shown in Fig. 8 the chemical requirements cannot be fulfilled at all chamber oxygen contents.

In Fig. 12 the metallographic cross sections of samples welded at low (200 ppm) and high (6000 ppm) chamber

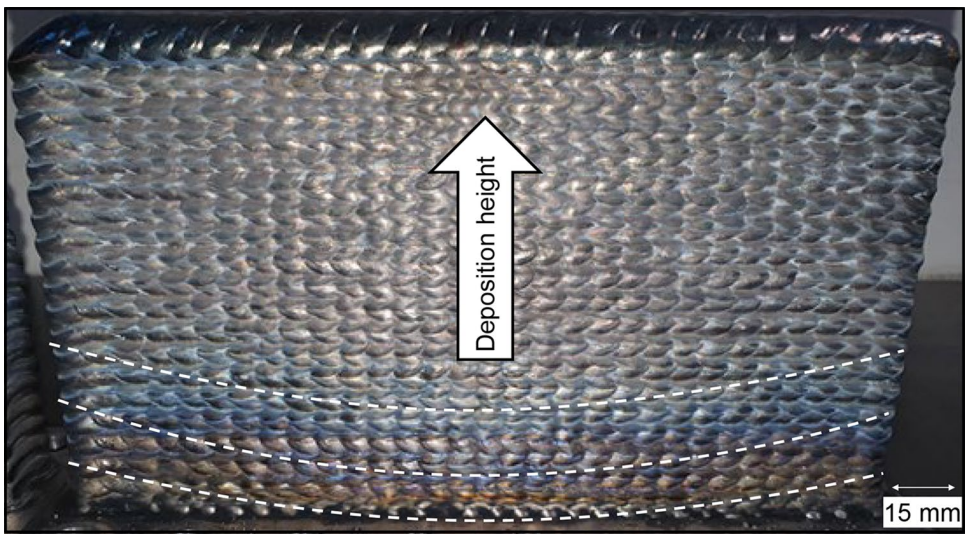

Fig. 7 Visual discolorations depending on the deposition height

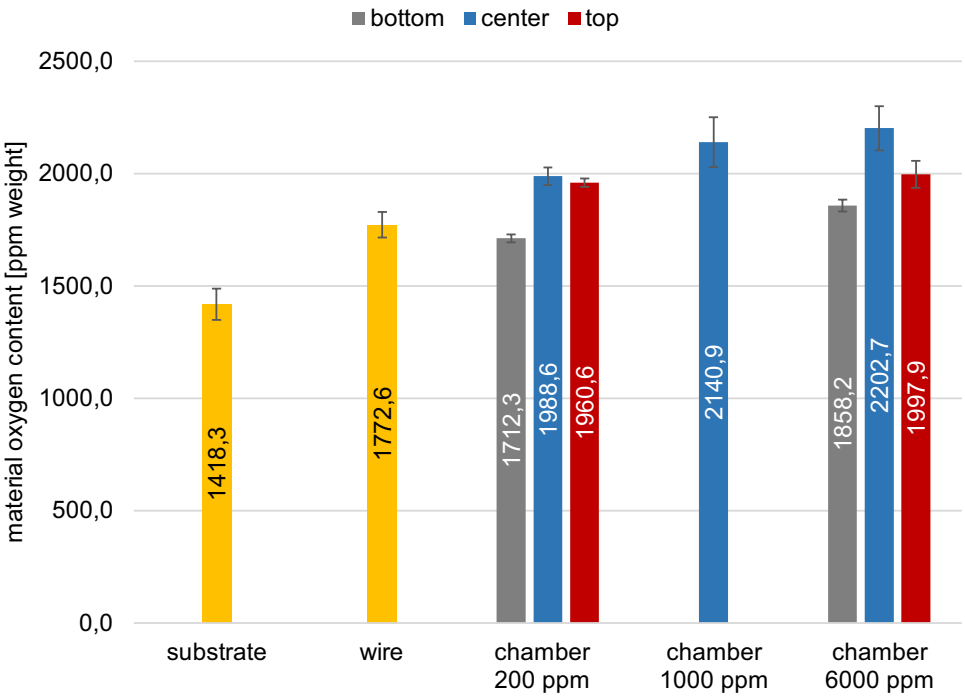

Fig. 8 Oxygen content in substrate material, wire material, and material of the samples welded at different chamber oxygen content measured at different heights

oxygen contents are shown. Both cross sections exhibit the same macroscopic structure showing large epitaxial prior β-grains and layer bandings. When comparing the microstructure at the surface of the deposit an α-case can be observed in the sample welded at high chamber oxygen content (6000 ppm). This α-case indicates an increasing oxide layer on the surface of the material and a proceeded oxygen diffusion close to the surface. The α-case has a maximum thickness of ≤ 84 µm at the sidewalls and ≤ 27 µm at the top surface of the last layer.

Metallographic cross sections of samples welded on pre-oxidized substrate material are shown in Fig. 13. Both samples show an α-case in the substrate material, while the sample oxidized using a high laser scanner speed (1100 mm/s) shows a smaller α-case compared to the sample oxidized using low laser scanner speed (300 mm/s). It can be observed in both samples, that the α-case dissolves when being welded on. A small area of α-case at the end of the weld cannot be dissolved. In the specimen with thicker α-case (300 mm/s laser scanning velocity) of ≤ 31 µm, it can be observed that occasionally the α-case seems to break off, move within the melt pool, and not being dissolved completely. However, the break-off α-case was only located close to the fusion line.

In Fig. 14, the weld when welding on preoxidized substrate material is shown, which is comparable to subsequently welding on an oxidized layer. Single bead deposition was chosen over oscillated deposition as it is more

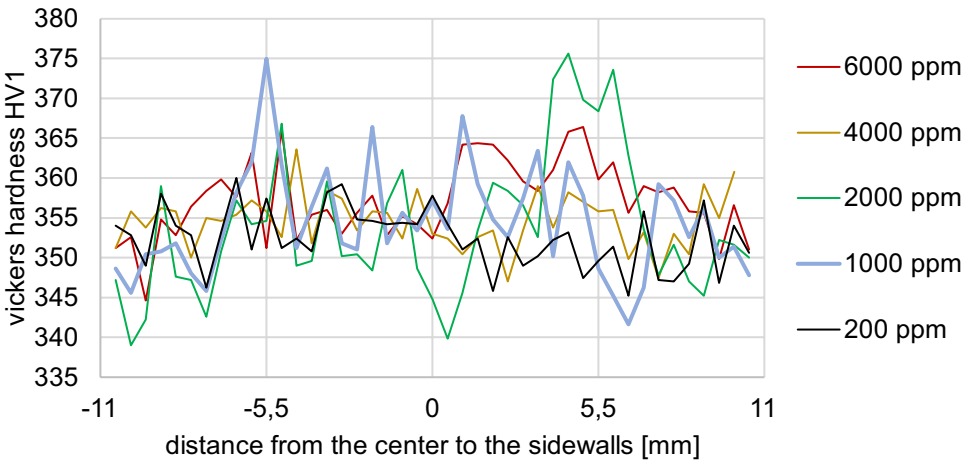

Fig. 9 Hardness profile along the width of the welded samples in dependence of the chamber oxygen content

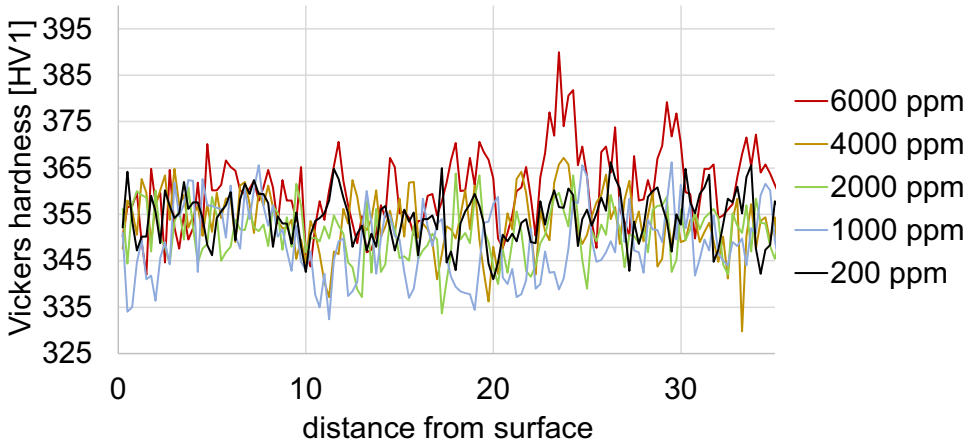

Fig. 10 Hardness profile along the height of the welded samples in the center of the in dependence of the chamber oxygen content

prone to possible arc instabilities due to the preoxidation of the substrate surface. Excluding weld start and end, the layer width and height stays constantly at 5.6 ± 0.2 mm and 2.5 ± 0.1 mm along the weld when welding preoxidized and non-preoxidized substrate material.

4 Discussion

As to be assumed, the average chamber oxygen content increases with higher ArO_2 98/2 gas flow. The recurring periodic decrease of oxygen content is linked to the additional ArHe 30/70 shielding gas flow from the welding torch. Upon finishing the post-flow time after each layer, the additional ArHe 30/70 shielding gas flow from the welding torch ceases and the oxygen content rises again due to the oxygen levels from the ArO_2 98/2 shielding gas flow. This periodical decrease and increase of the oxygen content decisively leads to a stationary state. The average oxygen content slowly decreases before reaching this stationary state, which can be linked to the increasing temperature accumulation over the welding time. Higher temperatures and longer exposure times at elevated temperatures lead to an increased oxygen pick-up of the deposited material, which decreases the oxygen content measured in the shielding gas chamber.

Depending on the oxygen content in the shielding gas chamber, the visual discolorations of the welded samples change according to the visual discolorations of titanium known from the literature [17]. This indicates an increased thickness of oxide layers on the welded samples with higher oxygen content in the shielding gas chamber. The different visual discolorations along the deposition height indicate, that the temperature field is not homogenous along the welded sample, which has been confirmed by Yang et al. [18]. Judging by the visual discolorations, the oxide layer increases along the deposition height, which seems to be linked to the temperature accumulation in the welded sample due to the poor thermal conductivity of Ti-6Al-4V and the high heat input of the WAAM process. When investigating the visual discolorations perpendicular to the deposition height, the center shows increased oxidation compared to the start and ending points of the welded sample. This indicates a higher temperature or a longer exposure time at elevated

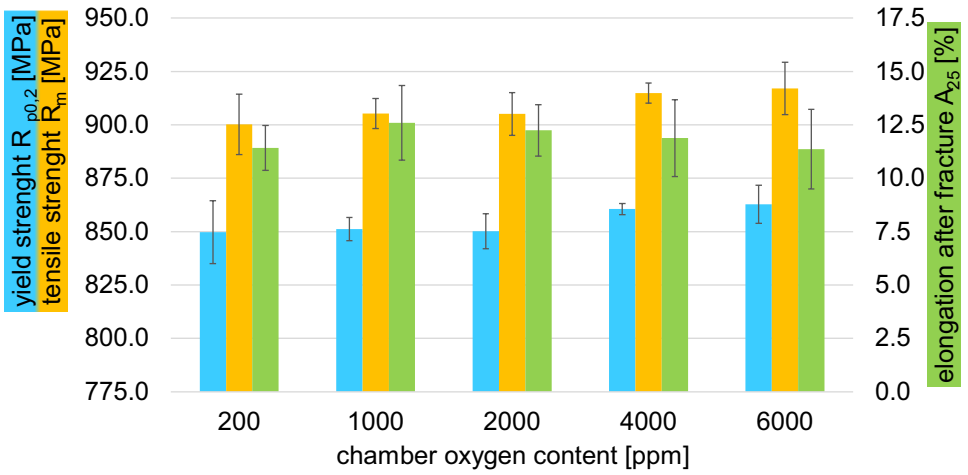

Fig. 11 Mechanical properties in dependence of the chamber oxygen content with requirements from aerospace industry indicated by dashed lines

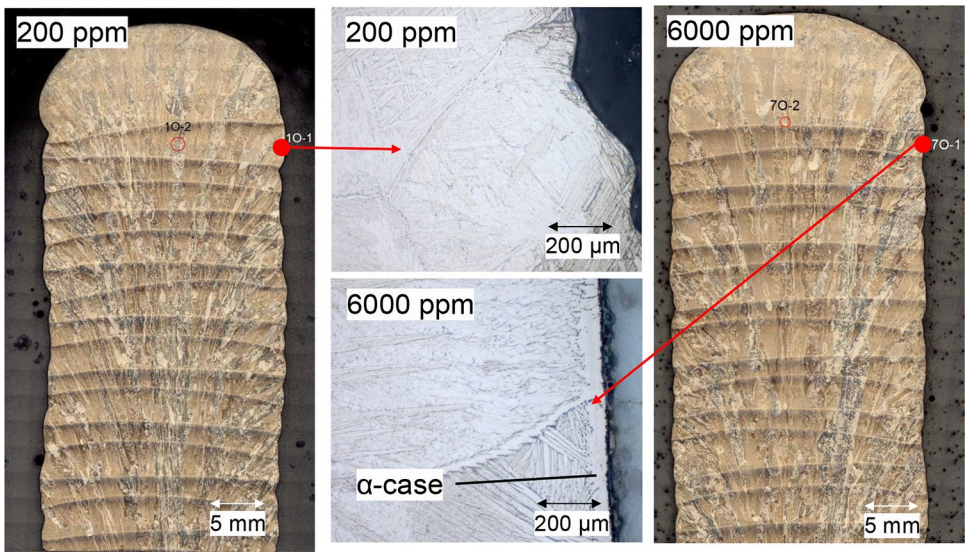

Fig. 12 Metallographic cross sections of samples welded at different chamber oxygen contents

temperatures in the center of the sample, which leads to an increased oxidation due to a higher diffusion coefficient and a longer oxidation time.

As judged by the visual discolorations, the material oxygen content measured with hot gas extraction increases over the deposition height, which is likely linked to increased temperature accumulation with deposition height. The oxidation at the top of the sample is lower compared to the center of the sample due to the reduced heat input by missing subsequent layers and therefore decreased oxidation. The lower material oxygen content close to the substrate (bottom) can be linked to the low temperature in the first layers due to the high thermal gradient to the cold substrate material. Moreover, a mixing of the deposit melt pool with the substrate material, which contains lower material oxygen content, can decrease the material oxygen content in the first layers. Even when welding at low chamber oxygen content (200 ppm) the material oxygen content increases by up to 216 weight ppm. This can be explained by the high oxidation affinity of Ti-6Al-4V [13]. When comparing this study to the state of the art [8–10], the high welding current and voltage as well as the usage of ArHe 30/70 torch shielding gas leads to a high deposit temperature and longer exposure times of the deposit to oxygen at elevated temperatures, which leads to an increased oxidation.

When drastically increasing the chamber oxygen content (6000 ppm), the material oxygen content only increases moderately, which indicates a decreased material oxidation due to a reduced diffusion of oxygen through the existing and growing TiO_2- and Al_2O_3-layer [13]. After a strong initial oxidation rate, the further oxidation rate decreases leading to moderate oxygen pick-up even at high oxygen content in the shielding gas atmosphere. However, the chemical requirements of the ASTM Grade 5 Titanium standards limit the maximum allowed oxygen content in the material to 2000 weight ppm, which is exceeded. To reach the chemical requirements of ASTM Grade 5 Titanium, a possible outlook for further investigation will be the study of the Titanium Grade 23—Ti-6Al-4V ELI (Extra Low Interstitials) wire welded in oxygen-rich shielding gas atmosphere. Ti-6Al-4V ELI welding wire is already standardized for aerospace and contains a lower content of oxygen of up to 800 weight ppm, which allows more oxidation due to an oxygen-rich shielding gas atmosphere until the maximum allowed content of

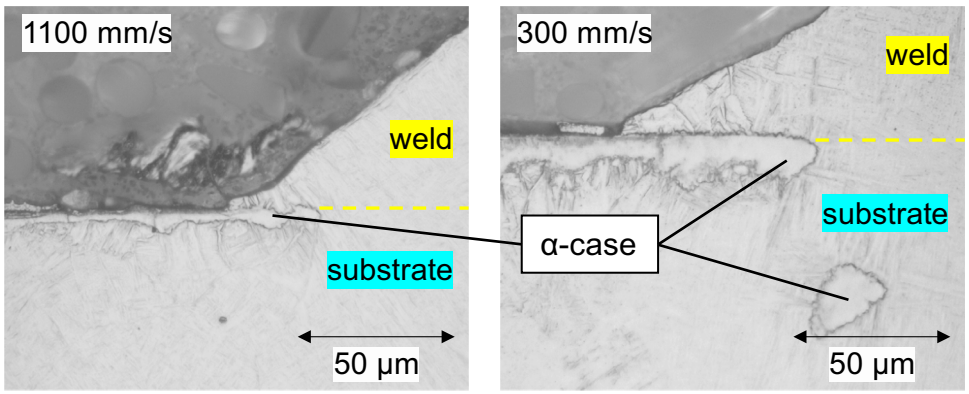

Fig. 13 Metallographic cross sections of samples welded on pre-oxidized substrate material in dependence on the laser scanner speed resulting in different α-layer thickness

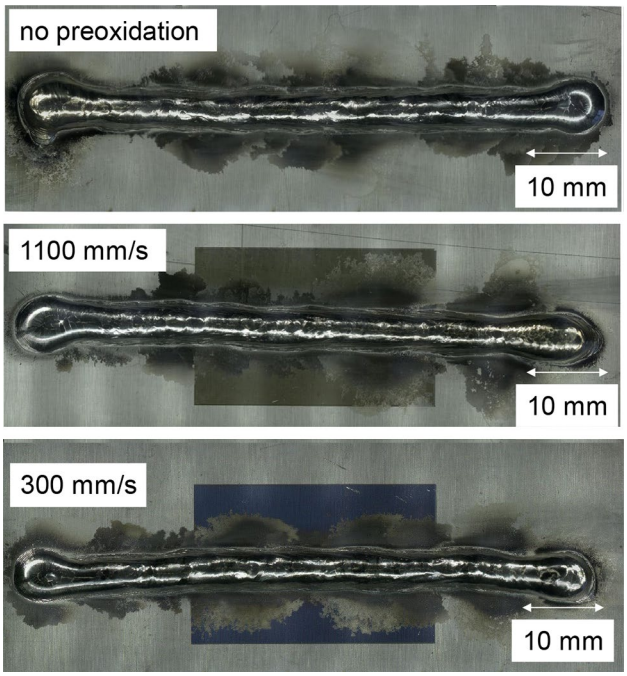

Fig. 14 Weld geometry in dependence on the preoxidation of the substrate material

2000 weight ppm according to ASTM Grade 5 Titanium is reached. Due to the reduced diffusion of oxygen, even local shielding concepts, which in most cases provide reduced shielding of oxygen, when compared to shielding gas chambers, will be viable.

The low chamber oxygen content of 200 ppm is not sufficient to increase the oxygen content at the surface enough to stabilize the α-titanium phase and forms α-case. On the contrary, when welding at high chamber oxygen content of 6000 ppm α-case develops at the surface of the layer. The maximum α-case thickness of ≤ 84 µm at the side walls of the samples is of no concern, since at least 1 mm of material is milled off afterwards following the process chain. This finding is consistent with the results of Caballero et al. [10], who found a resulting maximum α-case thickness of 70 µm or 200 µm when changing welding parameters. Unlike the sidewalls, the top of each layer is welded over by the subsequent layer and cannot be milled off. As shown in Fig. 8 the resulting increase of material oxygen content is moderate. Most of the oxygen responsible for the formation of the α-case dissolves when being welded over. However, as shown in Fig. 13 oxygen saturated α-titanium fragments can break off, move through the melt pool, and remain partially unmolten. These fragments pose a threat of a metallurgical notch and should be avoided. However, they were located close to the fusion line, which is milled off afterwards. Unlike the maximum α-case thickness at the side walls, which grew due to heat treatment of subsequent layers, the α-case thickness of the top layer is thinner, which reduces the risk of remaining α-case fragments. Aside of the rarely occurring remaining α-case fragments, the α-case as well as the oxide layer on the surface of the pre-oxidized substrate material is dissolved completely in the melt pool of the subsequent layer and does not represent a metallurgical notch. Additionally, the weld geometry is not influenced when welding on pre-oxidized surfaces, which indicates a stable deposition process and arc conditions even when welding on oxidized substrate or layers.

Even though the oxygen of the α-case and the oxide layer from the previously welded layer dissolve in the melt pool, the moderate periodical increase of hardness along the deposition height of samples welded at high chamber oxygen content indicates a local change in material oxygen content along the deposition height. This means the diffusion lengths are too short to fully equalize the material oxygen content in the bulk material neither during welding nor heat treatment. The same observation is shown when investigating the hardness profiles perpendicular to the deposition height. The uniform hardness profiles along the width of the deposit indicate a homogenous distribution of oxidation along the width of each layer. The oxygen from the α-case of the sidewalls seems to stay located close to the sidewall surface. The possible increases of hardness close to the surface could not be measured by the used method. However, this appears to be irrelevant since the sidewall surface will be milled off following the process chain.

The trend of increasing yield and tensile strength as well as decreasing elongation after fracture when welding at high chamber oxygen content was expected to follow the state of art [12]. An increasing scattering in the tensile properties at high chamber oxygen content can be related to the periodical increase in hardness along the sample height. However, the influence of high chamber oxygen content on the tensile properties is low, which seems to be linked to the parabolically decreasing oxidation rate over time due to the diffusion of oxygen through the growing oxide layer. Even though the requirements of the aerospace industry regarding the tensile properties are met, it needs to be noted, that in this work the chemical oxygen limits auf ASTM grade 5 titanium cannot be met. This, however, can be linked to the high material oxygen content in the wire feedstock.

5 Conclusion

In this study, the effects of different oxygen content in the shielding gas chamber on visual discoloration, oxygen content of the bulk material, microstructure, hardness profiles, and tensile properties of Ti-6Al-4V components produced by WAAM were investigated. The main findings are as follows:

- The chamber oxygen content reaches a steady level over the weld time and is affected by the increasing tempera-

ture of the deposit, resulting in chamber oxygen content between > 100 ppm and 6796 ppm depending on the additional ArO_2 98/2 gas flow.

- The visual inspection shows an increasing oxide layer thickness over the deposition height and in dependency of the chamber oxygen content with discolorations ranging from metallic silver, blue-violet, light blue to matt gray.
- The material oxygen content changes along the deposition height. Even at low chamber oxygen content there is a moderate increase of material oxygen content in the bulk material of up to 1961 ppm compared to the 1771 ppm contained in the wire. However, the further increase of material oxygen content when welding at high chamber oxygen content of 6000 ppm is comparably low with up to 2203 ppm, which can to be linked to the parabolic oxidation rate behavior of Ti-6Al-4V.
- Only at high chamber oxygen content α-case is formed on top (≤ 84 µm) and on the sidewalls (≤ 27 µm) of the samples. The thicker α-case on the sidewalls is milled off, while the thinner α-case on top of the layer dissolves after being welded over subsequently.
- The majority of the hardness profiles in and perpendicular to deposition height show an uniform average hardness of 353 HV1 regardless of the chamber oxygen content. However, welding at high chamber oxygen content leads to a moderate periodical increase of hardness along the deposition height of around 15 HV1. The periodical hardness increase is presumably related to the localized increase of material oxygen content by welding over previously oxidized layers.
- An increasing yield up to 863 MPa and tensile strength up to 917 MPa as well as decreasing elongation after fracture down to 11.4% is observed when welding the higher the chamber oxygen content. A deviation of this trend for specimen welded at low oxygen chamber content, which show a lower elongation after fracture, is under further investigation. The aerospace requirements on tensile properties can be reached even at high chamber oxygen levels of 6000 ppm. However, the chemical requirements of a maximum of 2000 ppm are exceeded. The influence of the chamber oxygen content on the tensile properties is moderate.

These findings lead to the conclusion, that in consideration of the known embrittling effect of pure oxygen in titanium alloys, the effect on the tensile properties along the deposition height of the WAAM deposit is moderate. Therefore, the oxygen content allowable in shielding gas chambers is higher as expected, which allows a decreased expense in chamber shielding. Additionally, the chamber oxygen content can be used to tailor the tensile properties of the deposit. While this study showed that the influence of pure oxygen on the tensile properties of Ti-6Al-4V is low, the influence of the material oxygen content on fatigue performance needs further investigation.

Regarding an economical and scalable WAAM process, a change from chamber to local shielding seems unavoidable. However, when using local shielding besides the moderate effect of oxygen alone also the embrittling effect of nitrogen and hydrogen needs to be considered.

Author contribution All authors contributed to the study conception and design. Material preparation, data collection, and analysis were performed by C. Halisch, B. Milcke, T. Radel, R. Rentsch. The first draft of the manuscript was written by C. Halisch and all authors commented on previous versions of the manuscript. All authors read and approved the final manuscript.

Funding Open Access funding enabled and organized by Projekt DEAL. The funding by the Federal Ministry for Economic Affairs and Climate Action BMWK (Grand Nr. 20W1708F and 20W1708C) on the basis of a decision of the German Bundestag is gratefully acknowledged.

Availability of data and material Our work has data included as supplementary material.

Code availability No code was developed in our work.

Declarations

Ethics approval All rules of good scientific practice have been applied for this publication.

Consent to participate My co-authors and I would not like to benefit from the participation on "In Review."

Consent for publication We agree with the Copyright Transfer Statement and wish to publish our work open access.

Competing interests The authors declare no competing interests.

References

1. Li S, Li JY, Jiang ZW, Cheng Y, Li YZ, Tang S, Leng JZ, Chen HX, Zou Y, Zhao YH, Oliveira JP, Zhang Y, Wang KH (2022) Controlling the columnar-to-equiaxed transition during directed energy deposition of inconel 625. Addit Manuf 57:102958

2. Ramalho A, Santos TG, Bevans B, Smoqi Z, Rao P, Oliveira JP (2022) Effect of contaminations on the acoustic emissions during wire and arc additive manufacturing of 316L stainless steel. Addit Manuf 51:102585
3. Ke WC, Oliveira JP, Cong BQ, Ao SS, Qi ZW, Peng B, Zeng Z (2022) Multi-layer deposition mechanism in ultra high-frequency pulsed wire arc additive manufacturing (WAAM) of NiTi shape memory alloys. Addit Manuf 50:102513
4. Rodrigues TA, Bairrão N, Farias FW, Shamsolhodaei A, Shen J, Zhou N, Maawad E, Schell N, Santos TG, Oliveira JP (2022) Steel-copper functionally graded material produced by twin-wire and arc additive manufacturing (T-WAAM). Mater Des 213:110270
5. Lütjering G, Williams JC (2007) Titanium. 2. Aufl. s.l. : Springer-Verlag
6. Wang F, Williams S, Colegrove P, Antonysamy A (2013) Microstructure and mechanical properties of wire and arc additive manufactured Ti-6Al-4V. Metall Mater Trans A 44(2):968–977
7. Bermingham MJ, Thomson-Larkins J, St John DH, Dargusch MS (2018) Sensitivity of Ti-6Al-4V components to oxidation during out of chamber Wire + Arc Additive Manufacturing. J Mater Process Technol 258:29–37
8. Elmer JW, Gibbs G (2019) The effect of atmosphere on the composition of wire arc additive manufactured metal components. Sci Technol Weld Join 24(5):367–374
9. Ding J, Colegrove P, Martina F, Williams S, Wiktorowicz R, Palt MR (2015) Development of a laminar flow local shielding device for wire + arc additive manufacture. J Mater Process Technol 226:99–105
10. Caballero A, Ding J, Bandari Y, Williams S (2018) Oxidation of Ti-6Al-4V during wire and arc additive manufacture. 3D Print Addit Manuf
11. Vaché N, Cadoret Y, Dod B, Monceau D (2021) Modeling the oxidation kinetics of titanium alloys: review, method and application to Ti-64 and Ti-6242s alloys. Corros Sci 178:109041
12. Leyens C, Peters M (2003) Titan und titanlegierungen. Wiley-VCH, Weinheim
13. Dong E, Yu W, Cai Q, Cheng L, Shi J (2017) High-temperature oxidation kinetics and behavior of Ti–6Al–4V Alloy. Oxid Met 88(5–6):719–732
14. Harwig DD, Fountain C, Ittiwattana W, Castner H (2000) Oxygen equivalent effects on the mechanical properties of titanium welds. AWS Weld J 305–316
15. Scotti FM, Teixeira FR, da Silva LJ, de Araujo DB, Reis RP, Scotti A (2020) Thermal management in WAAM through the CMT Advanced process and an active cooling technique. J Manuf Process 57:23–35
16. Halisch C, Gaßmann C, Seefeld T (2021) Investigating the reproducibility of the wire arc additive manufacturing process. Adv Mater Res 1161:95–104
17. Li X, Xie J, Zhou Y (2005) Effects of oxygen contamination in the argon shielding gas in laser welding of commercially pure titanium thin sheet. J Mater Sci 40(13):3437–3443
18. Yang D, Wang G, Zhang G (2017) Thermal analysis for single-pass multi-layer GMAW based additive manufacturing using infrared thermography. J Mater Process Technol 244:215–224